Dyes and Pigments 92 (2012) 909–915

Contents lists available at ScienceDirect

Dyes and Pigments

journal homepage: www.elsevier.com/locate/dyepig

A naphthalimide–rhodamine ratiometric fluorescent probe for Hg^{2+} based on fluorescence resonance energy transfer

Yunlong Liu, Xin Lv, Yun Zhao, Maliang Chen, Jing Liu, Pi Wang, Wei Guo*

School of Chemistry and Chemical Engineering, Shanxi University, Taiyuan 030006, China

ARTICLE INFO

Article history:
Received 25 June 2011
Received in revised form
24 July 2011
Accepted 25 July 2011
Available online 4 August 2011

Keywords:
Fluorescent probe
Ratiometric
Naphthalimide
Rhodamine
Desulfurization
Mercury ion

ABSTRACT

On the basis of fluorescent resonance energy transfer from 1,8-naphthalimide to rhodamine B, a new fluorophore dyads (**4**) containing rhodamine B and a naphthalimide moiety was synthesized as a ratiometric fluorescent probe for detecting Hg^{2+} with a broad pH range 5.7–11.0. The selective fluorescence response of **4** to Hg^{2+} is due to the Hg^{2+}-promoted desulfurization of the thiocarbonyl moiety, leading to the ring-opening of rhodamine B moiety of **4**. When **4** was employed at 0.1 μM with the slit size being 20 nm/20 nm, a low level of Hg^{2+} (up to 3×10^{-8} M) can be detected using the system.

1. Introduction

Mercury is the third most frequently found and second most common toxic heavy metal in the list of the Agency for Toxic Substances and Disease Registry (ATSDR) of the U.S. Department of Health and Human Services [1,2]. The extreme toxicity of mercury and its derivatives results from its high affinity for thiol groups in proteins and enzymes, leading to the dysfunction of cells and consequently causing health problems [3–5]. Unfortunately, mercury contamination can occur through a variety of natural and anthropogenic sources including oceanic and volcanic emissions, gold mining, and combustion of fossil fuels. Thus, the health concerns over exposure to mercury have motivated the exploration of selective and efficient methods for the monitoring of mercury in biological and environmental samples.

Fluorescence spectroscopy has become a powerful tool for sensing and imaging trace amounts of species such as metal ions because of its simplicity and high sensitivity [6–9]. The most reported fluorescent sensors display an increase or decrease in the emission intensity upon binding to species of interest. As the change in fluorescence intensity is the only detection signal, factors such as instrumental efficiency, environmental conditions, and the probe concentration can interfere with the signal output. To eliminate those effects, a ratiometric fluorescent measurement is desirable [10–14]. This technique uses the ratio of the fluorescent intensities at two different wavelengths, and provides a built-in correction for environmental effects, and stability under illumination, allowing precise and quantitative analysis and imaging even in complicated systems.

Several signaling mechanisms, such as intramolecular charge transfer (ICT) [15–18], excimer/exciplex formation [19–22], and fluorescence resonance energy transfer (FRET) [23–28], can be employed for the design of ratiometric measurement. Among them, FRET is a nonradiative energy transfer process in which the excitation energy of the donor is transferred to the nearby acceptor via long-range dipole–dipole interaction and/or short-range multipolar interaction. Although the efficiency of energy transfer is affected by the distance between the donor and the acceptor as well as the relative orientation of transition dipoles of both the donor and acceptor, it is mainly determined by the extent of the spectral overlap between the donor emission and acceptor absorption [29]. Therefore, it would be possible to fabricate a ratiometric probe based on the FRET mechanism if a molecule could generate a suitable fluorescent energy acceptor by the interaction with target analyte. In addition, because the pseudo-Stokes shifts of FRET-based probes are larger than the Stokes shifts of either the donor or acceptor dyes, thus, the possible self-quenching as well as fluorescence detection errors due to backscattering effects from the

* Corresponding author. Tel./fax: +86 351 7011600.
E-mail address: guow@sxu.edu.cn (W. Guo).

0143-7208/$ – see front matter © 2011 Elsevier Ltd. All rights reserved.
doi:10.1016/j.dyepig.2011.07.020

excitation source will be efficiently avoided [30]. However, despite many advantages, examples of the ratiometric fluorescence probes for Hg^{2+} based on FRET are considerably limited [31–34].

On the basis of the spirolactam (nonfluorescent) to ring-open amide (fluorescent) equilibrium of rhodamine, rhodamine-based dyes have been demonstrated to be excellent OFF/ON-type fluorescence probes [35,36]. On the other hand, 1,8-naphthalimide derivatives are excellent fluorophores due to their high stability and quantum yield as well as convenient functionalization at 4-position or imine site, and have been widely exploited as fluorescent probes [37–44]. Recently, two independent energy transfer dyads, both of which combine the properties of 1,8-naphthalimide and rhodamine dyes in a donor–acceptor chemical architecture for excited state energy transfer, were exploited as fluorescence ratiometric and turn-on probes for Cr^{3+} [25] and Hg^{2+} [45], respectively. Inspired by these results as well as the Hg^{2+}-induced desulfurization reactions [46–49], in this paper we hope to report a new naphthalimide–rhodamine ratiometric fluorescent probe for Hg^{2+} based on FRET. The strategy for FRET detection of Hg^{2+} is based on modulating the FRET process in a fluorophore dyads (**4**) comprising a 1,8-naphthalimide donor and a rhodamine-thiosemicarbazide acceptor linked by a rigid phenyl spacer (Fig. 1). In the absence of Hg^{2+}, the rhodamine moiety adopts a closed, non-fluorescent spirolactam form, thus, FRET is suppressed, and only the yellow emission of the donor is observed upon excitation of the 1,8-naphthalimide donor. In the presence of Hg^{2+}, the Hg^{2+}-promoted reaction of thiosemicarbazide to oxadiazole will induce opening of the rhodamine moiety [46], and produces intense rhodamine absorption in the 1,8-naphthalimide emission region. Therefore, excitation of the 1,8-naphthalimide chromophore results in strong red emission of rhodamine due to FRET.

2. Experiment

2.1. Materials and general methods

4-Morpholin-1,8-naphthalic anhydride (**1**) [50] and rhodamine B hydrazine [51] were prepared by literature procedures. All other reagents and solvents were purchased from commercial sources and were of the highest grade. Solvents were dried according to standard procedures. All reactions were magnetically stirred and monitored by thin-layer chromatography (TLC). Flash chromatography (FC) was performed using silica gel 60 (230–400 mesh). Absorption spectra were taken on an Agilent 8453 spectrophotometer. Fluorescence spectra were taken on HITACHI F-2500 fluorescence spectrometer. The ^1H NMR and ^{13}C NMR spectra were recorded at 300 and 75 MHz, respectively. The following abbreviations were used to explain the multiplicities: s = singlet; d = doublet; t = triplet; q = quartet; m = multiplet; br = broad. High resolution mass spectra were obtained on a Varian QFT-ESI mass spectrometer.

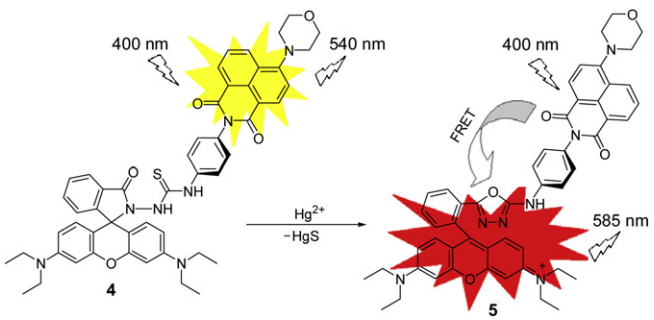

Fig. 1. The response mechanism of **4** to Hg^{2+}.

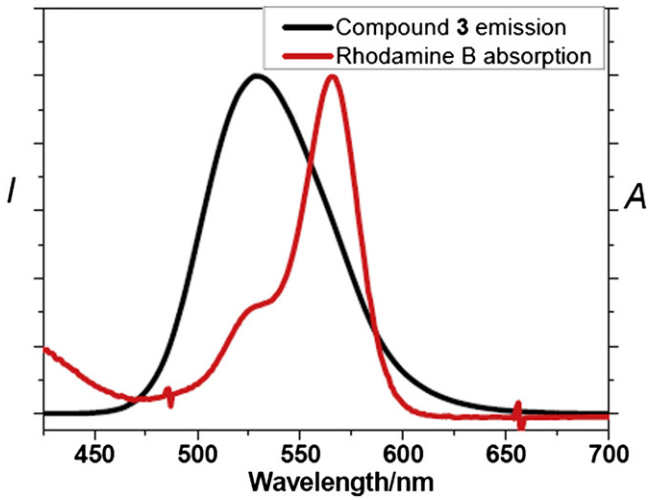

Fig. 2. Spectral overlap of the donor **3** emission with the acceptor rhodamine B absorption.

2.2. Synthesis

2.2.1. Compound 4

A solution of 4-morpholin-1,8-naphthalic anhydride (**1**, 0.1 g, 0.35 mmol) and *p*-phenylenediamine (0.76 g, 0.70 mmol) in ethanol (40 mL) was heated under reflux for 24 h. After left to cool, the precipitated crystals were filtered and washed with ethanol to give **2** as yellow solid (96 mg, 73%). Mp: 306–308 °C. ^1H NMR (300 MHz, DMSO-*d6*) δ 8.49 (d, J = 9.0, 1H), 8.44 (d, J = 6.9, 1H), 8.37 (d, J = 8.1, 1H), 7.80 (t, J = 7.8, 1H), 7.35 (d, J = 8.1, 1H), 6.88 (d, J = 7.2, 2H), 6.62 (d, J = 8.1, 2H), 5.19 (b, 2H), 3.90 (b, 4H), 3.21 (b, 4H).

A solution of **2** (0.1 g, 0.26 mmol) in CH_2Cl_2 (10 mL) was added slowly to a solution of thiocarbonyl chloride (75 μL, 0.1 mmol) in CH_2Cl_2 (12 mL) and NEt_3 (1 mL), and the mixture was stirred for 5 h at room temperature. Then the reaction mixture was washed with water, dried over Na_2SO_4, and evaporated under reduced pressure. The solid was purified on flash silica gel using CH_2Cl_2 as eluent to give **3** as yellow solid (97 mg, 90%). ^1H NMR (300 MHz, $CDCl_3$) δ 8.68 (d, J = 6.9, 1H), 8.63 (d, J = 8.1, 1H), 8.54 (d, J = 8.4, 1H), 7.82 (t, J = 8.1, 1H), 7.46–7.32 (m, 5H), 4.09 (b, 4H), 3.36 (b, 4H).

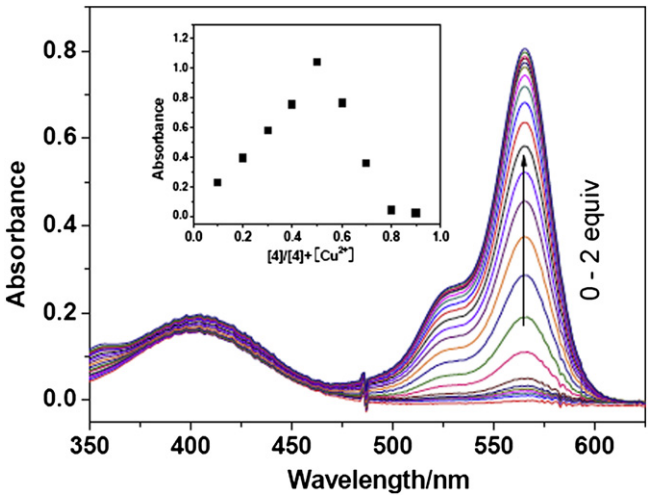

Fig. 3. Changes in absorption spectra of **4** (10 μM) in 2:1 (v/v) MeOH/water solution (10 mM Tris–HCl, pH 7.0) with various amounts of Hg^{2+} ions. Inset: Job's plot for determining the stoichiometry of **4** and Hg^{2+}.

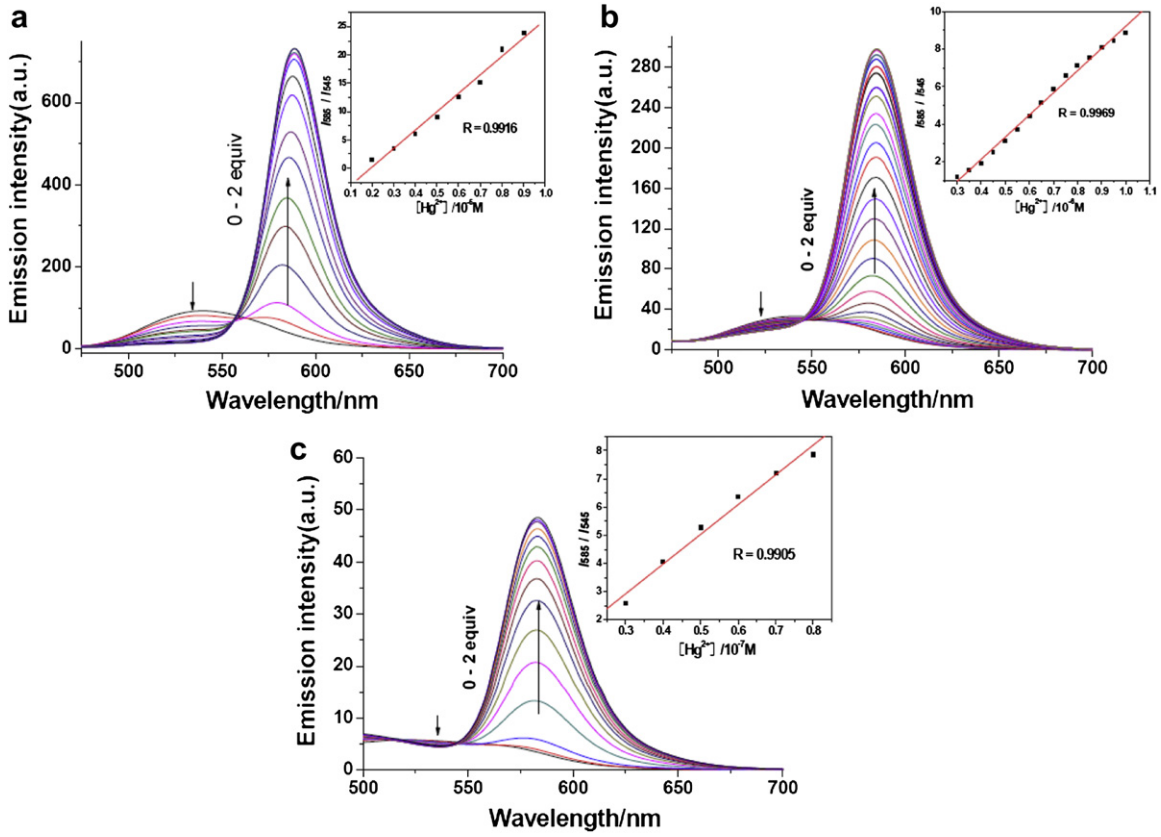

Fig. 4. Fluorescence titration spectra of **4** [10 μM, 1 μM, and 0.1 μM for (a), (b) and (c), respectively] in 2:1 (v/v) MeOH/water solution (10 mM Tris–HCl, pH 7.0) upon gradual addition of Hg^{2+}. Inset: Fluorescence intensity ratio changes (I_{585}/I_{545}) of **4** upon gradual addition of Hg^{2+}. $\lambda_{ex} = 400$ nm. Slits: 10 nm/10 nm for (a), 20 nm/20 nm for (b) and (c).

A stirred of solution of rhodamine B hydrazide (0.11 g, 0.24 mmol) and compound **3** (0.1 g, 0.24 mmol) in DMF was heated at 60 °C for 36 h. The solvent was evaporated at reduced pressure, and the residue was purified on flash gel using CH_2Cl_2/MeOH (10:1, v/v) as eluent to give **4** as yellow solid (95 mg, 45%). Mp: 242–244 °C. ^{1}H NMR (300 MHz, $CDCl_3$) δ 8.50 (m, 4H), 8.01 (b, 1H), 7.53–7.70 (m, 5H), 7.19–7.28 (m, 4H), 7.05–7.10 (m, 3H), 6.50 (d, $J = 8.1$, 2H), 6.44 (s, 1H), 6.32 (d, $J = 8.1$, 2H), 4.02 (b, 4H), 3.27–3.34 (m, 12H), 1.15 (t, J = 6.6, 12H). ^{13}C NMR (75 MHz, $CDCl_3$): 165.0, 164.6, 156.6, 154.9, 150.8, 150.0, 140.9, 138.5, 135.0, 133.6, 132.7, 132.2, 131.1, 130.9, 129.8, 129.3, 128.3, 126.8, 126.6, 125.4, 124.6, 124.0, 117.7, 115.7, 109.1, 104.8, 99.0, 67.6, 54.1, 46.5, 45.1, 13.3. TOF MS calcd. for $(M+H)^+$ 872.3516, found 872.3539.

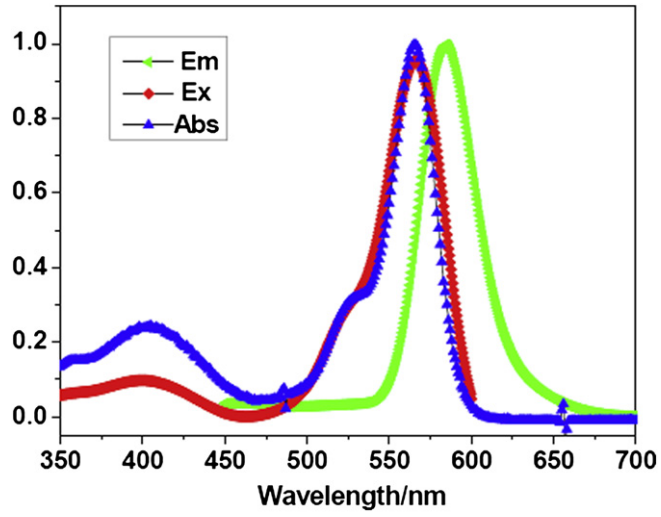

Fig. 5. Normalized excitation, absorption and emission spectra of **5** in 2:1 (v/v) MeOH/water solution (10 mM Tris–HCl, pH 7.0). The emission data were collected at 585 nm. The excitation wavelength is 400 nm.

2.2.2. Compound *5*

A mixture of compound **4** (87.2 mg, 0.1 mmol) and $Hg(NO_3)_2 \cdot H_2O$ (34.2 mg, 0.1 mmol) was stirred in MeOH for 10 min at room temperature. The solvent was evaporated under reduced pressure and the crude product was purified by column chromatography on silica gel using CH_2Cl_2/MeOH (20:1, v/v) as eluent to give **5** as red solid (77 mg, 91%). ^{1}H NMR (300 MHz, CDCl3): δ 11.14 (b, 1H), 8.40–8.52 (m, 3H), 8.22 (b, 1H), 7.89 (d, $J = 8.4$, 2H), 7.67 (m, 3H), 7.08–7.27 (m, 6H), 6.72–6.81 (m, 4H), 3.99 (b, 4H), 3.52 (b, 8H), 3.24 (b, 4H), 1.25 (b, 12H). ^{13}C NMR (75 MHz, $CDCl_3$): 165.0, 161.3, 158.9, 156.3, 139.7, 133.6, 132.3, 131.7, 131.2, 131.0, 129.8, 126.8, 124.4, 119.4, 118.1, 115.8, 115.0, 114.7, 97.3, 67.8, 54.3, 46.9, 13.5. TOF MS calcd. for $(M)^+$ 838.3717, found 838.3722.

2.2.3. Compound *6*

Compound **6** was synthesized according to the similar procedure to compound **4** except that phenyl isothiocyanate was used. ^{1}H NMR (300 MHz, DMSO-*d6*) δ 8.03 (d, 1H), 7.66–7.54 (m, 3H), 7.48 (s, 2H), 7.15(d, $J = 7.2$, 2H), 7.07 (d, $J = 2.1$, 3H), 6.95(d, $J = 3.6$, 1H), 6.75 (s, 1H), 6.48 (m, 3H), 6.31 (s, 1H), 3.33 (q, 8H), 1.15 (t, $J = 6.6$, 12H). ^{13}C NMR (75 MHz, $CDCl_3$): 183.2, 167.7, 154.8, 150.7, 149.8, 138.2, 134.8, 129.5, 128.8, 126.6, 125.6, 125.3, 124.4, 108.8, 104.7, 98.8, 67.7, 44.9, 13.1.

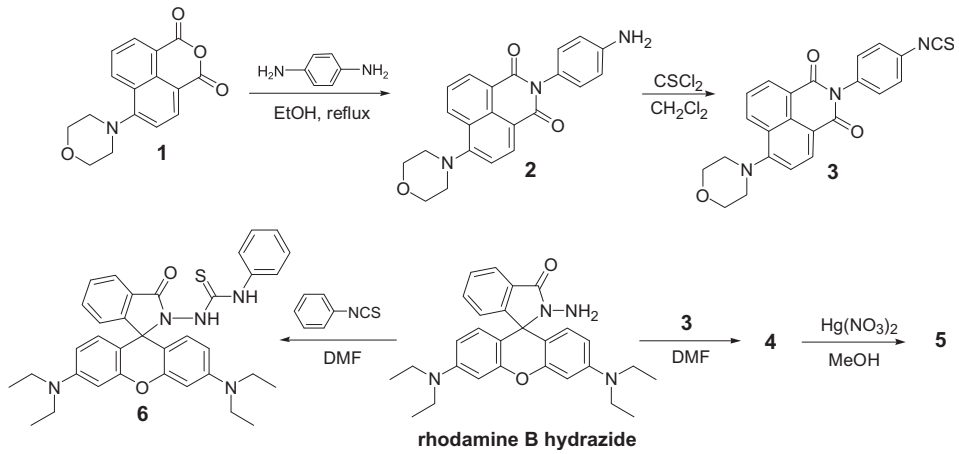

Scheme 1. Synthesis of compounds **4**, **5** and control compound **6**.

2.3. Procedures of ions sensing

Deionized water was used throughout all experiments. Solutions of Ca^{2+} and Au^{3+} were prepared from their chloride salts; solutions of Na^{+}, K^{+}, Ag^{+}, Mg^{2+}, Cu^{2+}, Cd^{2+}, Co^{2+}, Mn^{2+}, Ni^{2+}, Zn^{2+}, Hg^{2+}, Pb^{2+}, Cr^{3+}, and Fe^{3+} were prepared from their nitrate salts. Solution of $PdCl_2$ was prepared in 95:5 MeOH/Brine. A stock solution of **4** (1.25×10^{-2} M) was prepared in DMF. The stock solution of **1** was then diluted to the corresponding concentration (10 μM and 1 μM) with the 2:1 (v/v) MeOH/water solution (10 mM Tris–HCl, pH 7.0). The Hg^{2+} stock solution of 5.0×10^{-2} M was diluted to 1.0×10^{-2} M, 1.0×10^{-3} M and 1.0×10^{-4} M with deionized water for spectra titration studies. In the titration experiments, a 2.5 mL solution of **4** (10 μM and 1 μM) was poured into a quartz optical cell of 1 cm optical path length each time, and Hg^{2+} solution was added into the quartz optical cell gradually by using a micro-pipette. Spectra data were recorded in an indicated time after the addition.

3. Results and discussion

Compound **4** and its ring-opened product **5**, as well as a control compound **6** were efficiently synthesized and well characterized (see: Experimental section). As we know, the spectra overlap is the main factor that determines the efficiency of FRET. In the construction of FRET system of **4**, 1,8-naphthalimide fluorophore was chosen as an energy donor because it has strong emission in the visible range and its broad emission (450–650 nm) covers a part of rhodamine's absorption, fulfilling a favorable condition for FRET (Fig. 2). A 2:1 (v/v) MeOH/water solution (10 mM Tris–HCl, pH 7.0) was selected as a testing system to investigate the chemical response of **4** to Hg^{2+} at room temperature (about 20 °C). A time course of the absorption response of **4** upon addition of Hg^{2+} revealed the recognizing event could complete in 10 min, and remains quite stable from 10 to 50 min. Thus, a reaction time of 10 min was chosen for the present studies.

3.1. UV/Vis titration investigation

The UV/Vis spectrum of **4** showed only the absorption profile of the donor (1,8-naphthalimide), which has a maximum at 405 nm. Addition of Hg^{2+} ions induced an increase in the absorption intensity at 565 nm (Fig. 3), which corresponds to the absorption of rhodamine. The absorption stabilized after the amount of added Hg^{2+} ions

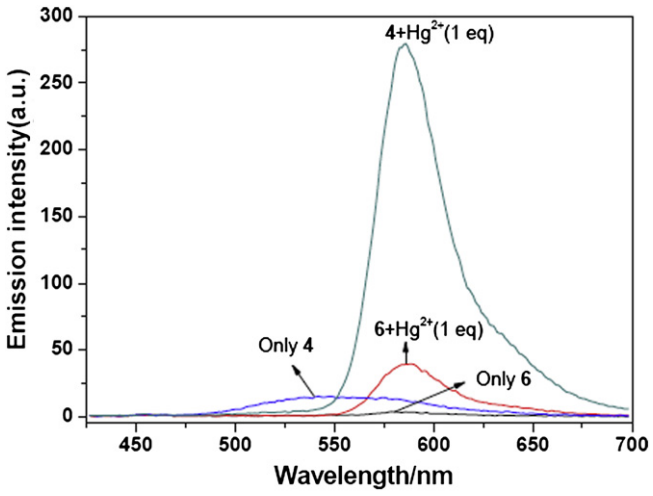

Fig. 6. Fluorescence titration spectra of **4** and **6** (both: 1 μM) in 2:1 (v/v) MeOH/water solution (10 mM Tris–HCl, pH 7.0) upon addition of Hg^{2+} (1 equiv). $\lambda_{ex} = 400$ nm. Slits: 20 nm/20 nm.

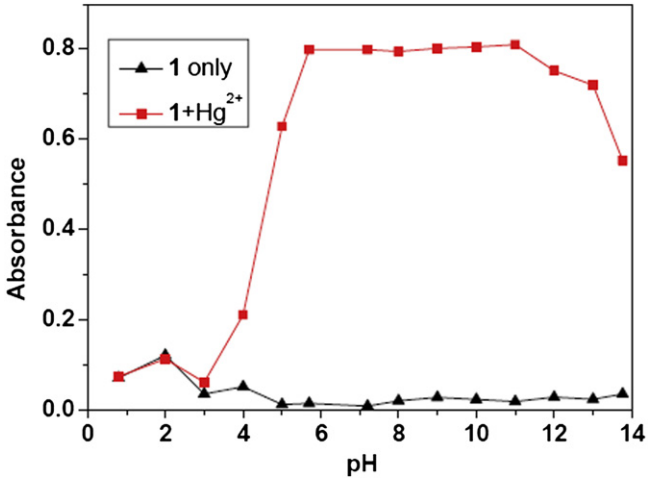

Fig. 7. Changes in absorption (565 nm) of **4** (10 μM) in 2:1 (v/v) MeOH/water solution measured with and without Hg^{2+} (1 equiv) as a function of pH. **4** + Hg^{2+} (red), **4** (black). (For interpretation of the references to colour in this figure legend, the reader is referred to the web version of this article.)

reached 1 equiv and a significant color change from colorless to red could be observed easily by eye, indicating that the addition of Hg^{2+} ions can promote the formation of the ring-opened compound **5**. Further evidence for the formation of **5** comes from the independent synthesis of **5** from **4** by using 1 equiv of $Hg(NO_3)_2$ in MeOH at room temperature (see: Experimental section). Job plot analysis of the UV–Vis titrations revealed a maximum at about 0.5 mole fraction (Fig. 3, inset), indicating 1:1 binding stoichiometry. Noteworthy is that in the titration process the 1,8-naphthalimide absorption at 405 nm was almost unchanged, and the absorption spectrum obtained after adding 1 equiv Hg^{2+} ions reflects the presence of the separate 1,8-naphthalimide and rhodamine B units, indicating that there are very weak electronic interactions between the donor and the acceptor in the ground state.

3.2. Fluorescence titration investigation

As shown in Fig. 4a, the free **4** (10 μM) displayed a weak 1,8-naphthalimide emission band centered at 540 nm when excited at 400 nm (excitation of 1,8-naphthalimide moiety). The weak fluorescence emission of naphthalimide unit of **4** is probably due to photo-induced electron transfer (PET) from the nitrogen atom of thiosemicarbazide moiety to the photoexcited naphthalimide moiety. Upon addition of Hg^{2+} the 1,8-naphthalimide emission decreased, and a new emission band centered at 585 (emission of rhodamine B moiety) appeared and gradually increased in intensity. The emission intensity stabilized after the amount of added Hg^{2+} ions reached 1 equiv with a well-defined isoemission point. The emission intensities at 585 nm and 545 nm (F_{585}/F_{545}) exhibited

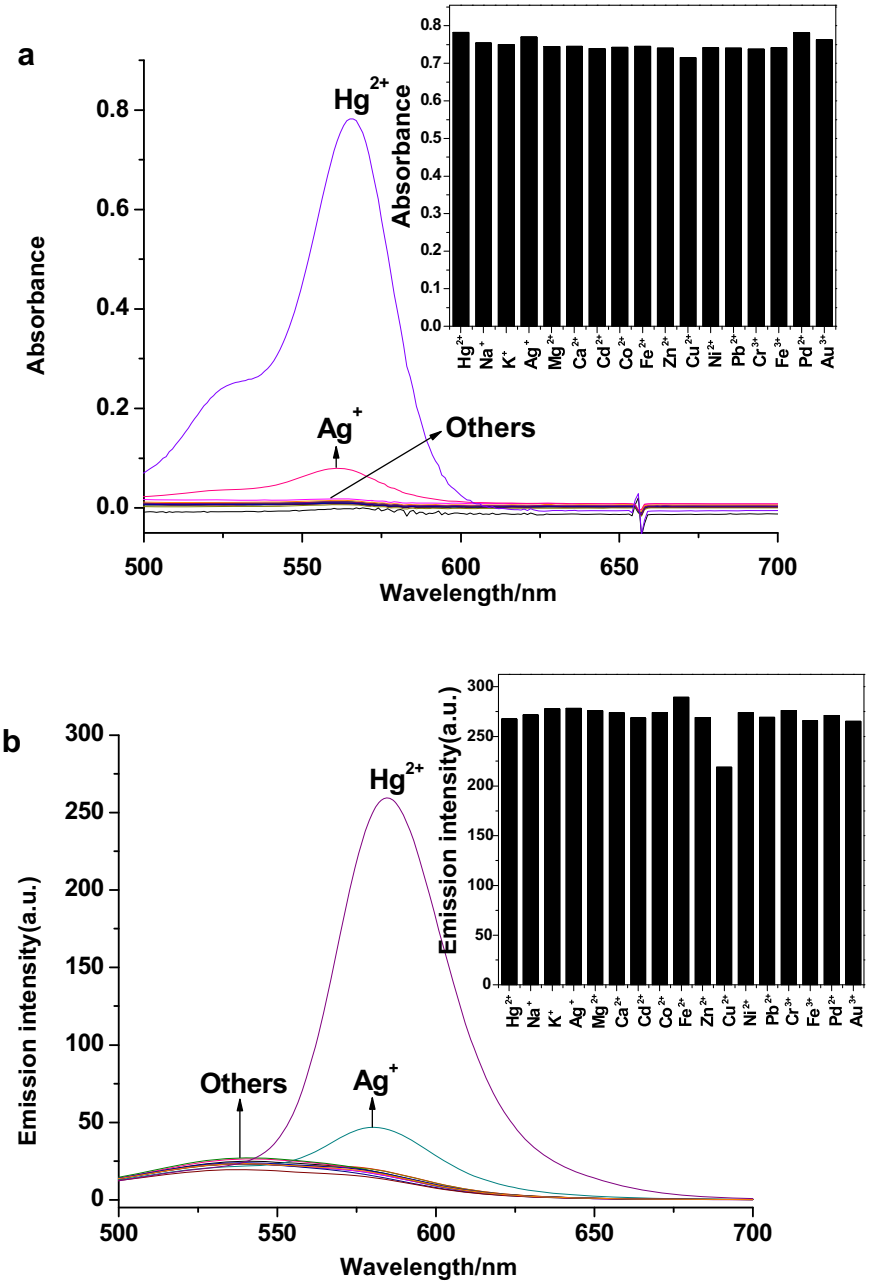

Fig. 8. The absorption (a) and fluorescence (b) spectra of **4** (10 μM and 1 μM, respectively) upon addition of 1 equiv of Hg^{2+} and various other metal ions, including of Na^{+}, K^{+}, Mg^{2+}, Fe^{2+}, Fe^{3+}, Cr^{3+}, Ca^{2+}, Zn^{2+}, Co^{2+}, Pb^{2+}, Cd^{2+}, Ni^{2+}, Ag^{+}, Au^{3+}, Pd^{2+} (10 equiv) and Cu^{2+} (1 equiv), in 2:1 (v/v) MeOH/water solution (10 mM Tris–HCl, pH 7.0). Inset: spectra response of **4** to Hg^{2+} containing various metal ions.

a big change from 0.44 in the absence of Hg^{2+} to 28.7 when the amount of Hg^{2+} ions added reached 1 equiv of **4**. A good linear working range from 2 to 10 μM was observed in the titration experiment. In addition, we also measured the sensitivity of **4** for monitoring the lower concentration of Hg^{2+} by changing the slit size. When **4** was employed at 1 μM with the slit size being 20 nm/20 nm, the good linear working range from 0.3 to 1 μM is obtainable (Fig. 4b). Further, when **4** was employed at 0.1 μM with the same slit size (20 nm/20 nm), the good linear working range from 0.03 to 0.08 μM can still be obtained (Fig. 4c), suggesting a lower level of Hg^{2+} can be detected using the system.

It was clear that the FRET process was switched on by Hg^{2+} ions as excitation of 1,8-naphthalimide at 400 nm resulted in the emission of rhodamine with a maximum of 585 nm. This can also be corroborated by the excitation spectra of the ring-opened product **5**. The excitation spectra obtained by collecting emission data of **5** at 585 nm shows both the donor and the acceptor bands with good correspondence with the absorption spectra (Fig. 5), indicating that both the two transitions participate in the emission process, and an efficient energy transfer can occur from the 1,8-naphthalimide donor to the rhodamine acceptor. The efficiency of energy transfer (EET) was calculated to be 86.3% based on the equation [52]: $\eta_{EET} = 1 - \Phi_{F(\text{donor in FRET system})}/\Phi_{F(\text{free donor})}$, in which η_{EET} is the efficiency of energy transfer, $\Phi_{F(\text{donor in FRET system})}$ is the fluorescence quantum yields of the donor part in FRET system (1,8-naphthalimide part in **5** in this investigation), and $\Phi_{F(\text{free donor})}$ is the fluorescence quantum yields of the donor when not connected to the acceptor (1,8-naphthalimide part in **4** in this investigation).

Further, to evaluate the role of the 1,8-naphthalimide donor moiety, a control compound **6** (with the 1,8-naphthalimide group in **4** being replaced by a phenyl group) was synthesized (Scheme 1) and its fluorescent response performances were investigated and compared with that of **4** in the same conditions. The free **6** displayed no any emission when excited at 400 nm (excitation of 1,8-naphthalimide). Upon addition of 1 equiv Hg^{2+}, only a weaker emission compared with **4** + Hg^{2+} was observed at 585 nm (Fig. 6). Obviously, the 1,8-naphthalimide donor plays an important role for FRET of **4** + Hg^{2+}. The property is especially important because a large Stokes shift (185 nm) can be realized in this system, which can eliminate any influence of excitation backscattering effects on the fluorescence assay and facilitate the practical application.

3.3. pH investigation

In addition, to apply **4** in more complicated systems, the spectra response of **4** in the absence and presence of Hg^{2+} in different pH values were evaluated (Fig. 7). Without Hg^{2+}, no obvious characteristic absorption of rhodamine could be observed for **4** between pH 5.7 and 11.0. Upon addition of Hg^{2+}, **4** responded stably to Hg^{2+} in the same region without any interference by protons. These results indicate that **4** successfully react with Hg^{2+} and allow Hg^{2+} detection in a wide pH range.

3.4. Selectivity investigation

An important feature of **4** is its high selectivity toward the Hg^{2+} over the other competitive species. Changes of fluorescence and UV/Vis spectra of **4** caused by Cu^{2+} and miscellaneous metal ions including Na^{+}, K^{+}, Mg^{2+}, Fe^{2+}, Fe^{3+}, Cr^{3+}, Ca^{2+}, Zn^{2+}, Co^{2+}, Pb^{2+}, Cu^{2+}, Cd^{2+}, Ni^{2+}, Ag^{+}, Au^{3+} and Pb^{2+} in 2:1 (v/v) MeOH/water solution (10 mM Tris–HCl, pH 7.0) are recorded in Fig. 8. Most of the competitive cations, except for Ag^{+}, which had a slight effect, did not lead to any significant fluorescence and absorption changes in the visible region. Moreover, in the presence of miscellaneous competitive metal ions, the Hg^{2+} ion still resulted in the similar fluorescence and absorption changes (Fig. 8, inset). In addition, because the excess of Cu^{2+} can partly quenches the fluorescence of **4** + Hg^{2+} due to its paramagnetic property, thus, only 1 equiv of Cu^{2+} was used in the selectivity experiment.

4. Conclusions

In summary, we have developed a new ratiometric fluorescent probe **4** for Hg^{2+} based on an intramolecular FRET with an excellent selectivity over other metal ions. It exhibits a clear Hg^{2+}-induced change in the intensity ratio of the two emission bands of naphthalimide and rhodamine. The selective absorption and fluorescence response of **4** is due to the Hg^{2+}-promoted desulfurization of the thiocarbonyl moiety, leading to the ring-opening of rhodamine B moiety of **4**. We expect that the method will serve as practical tool for environmental samples analysis and biological studies.

Acknowledgments

We would like to thank the Natural Science Foundation of China (NSFC Nos. 20772073 and 21072121) and the Natural Science Foundation of Shanxi Province (2008011015-2) for financial support.

References

[1] Patrick L. Mercury toxicity and antioxidants. Part 1. Role of glutathione and alpha-lipoic acid in the treatment of mercury toxicity. Altern Med Rev 2002;7:456–71.
[2] US EPA. Regulatory impact analysis of the clean air mercury rule. Final Report. EPA-452/R-05–003. Research Triangle Park, NC: US EPA; 2005.
[3] Grandjean P, Weihe P, White RF, Debes F. Cognitive performance of children prenatally exposed to “safe” levels of methylmercury. Environ Res 1998;77:165–72.
[4] Takeuchi T, Morikawa N, Matsumoto H, Shiraishi Y. A pathological study of Minamata disease in Japan. Acta Neuropathol 1962;2:40–57.
[5] Harada M. Minamata disease: methylmercury poisoning in Japan caused by environmental pollution. Crit Rev Toxicol 1995;25:1–25.
[6] Callan JF, de Silva AP, Magri DC. Luminescent sensors and switches in the early 21st century. Tetrahedron 2005;61:8551–88.
[7] Martínez-Máñez R, Sancanón F. Fluorogenic and chromogenic chemosensors and reagents for anions. Chem Rev 2003;103:4419–76.
[8] Czarnik AW. Chemical communication in water using fluorescent chemosensors. Acc Chem Res 1994;27:302–8.
[9] Kim JS, Quang DT. Calixarene-derived fluorescent probes. Chem Rev 2007;107:3780–99.
[10] Grynkiewicz G, Poenie M, Tsien RY. A new generation of Ca^{2+} indicators with greatly improved fluorescence properties. J Biol Chem 1985;260:3440–50.
[11] Tsien RY, Harootunian AT. Practical design criteria for a dynamic ratio imaging system. Cell Calcium 1990;11:93–109.
[12] Coskun A, Akkaya EU. Ion sensing coupled to resonance energy transfer: a highly selective and sensitive ratiometric fluorescent chemosensor for Ag(I) by a modular approach. J Am Chem Soc 2005;127:10464–5.
[13] Coskun A, Akkaya EU. Signal ratio amplification via modulation of resonance energy transfer: proof of principle in an emission ratiometric Hg(II) sensor. J Am Chem Soc 2006;128:14474–5.
[14] Lin W, Yuan L, Long L, Guo C, Feng J. A fluorescent cobalt probe with a large ratiometric fluorescence response via modulation of energy acceptor molar absorptivity on metal ion binding. Adv Funct Mater 2008;18:2366–72.
[15] Xu Z, Qian X, Cui J. Colorimetric and ratiometric fluorescent chemosensor with a large red-shift in emission: Cu(II)-only sensing by deprotonation of secondary amines as receptor conjugated to naphthalimide fluorophore. Org Lett 2005;7:3029–32.
[16] Yang H, Liu Z, Zhou Z, Shi E, Li F. Highly selective ratiometric fluorescent sensor for Cu(II) with two urea groups. Tetrahedron Lett 2006;47:2911–4.
[17] Liu Z, Zhang C, He W, Yang Z, Gao X, Guo Z. A highly sensitive ratiometric fluorescent probe for Cd^{2+} detection in aqueous solution and living cells. Chem Commun 2010;46:6138–40.
[18] Goswami S, Sen D, Das NK. A new highly selective, ratiometric and colorimetric fluorescence sensor for Cu^{2+} with a remarkable red shift in absorption and emission spectra based on internal charge transfer. Org Lett 2010;12:856–9.
[19] Kim JS, Choi MG, Song KC, No KT, Ahn S, Chang S-K. Ratiometric determination of Hg^{2+} ions based on simple molecular motifs of pyrene and dioxaoctanediamide. Org Lett 2007;9:1129–32.
[20] Kim H, Hong J, Hong A, Ham S, Lee J, Kim JS. Cu^{2+}-induced intermolecular static excimer formation of pyrenealkylamine. Org Lett 2008;10:1963–6.

[21] Jung H, Park M, Han D, Kim E, Lee C, Kim JS. Cu^{2+} ion-induced self-assembly of pyrenylquinoline with a pyrenyl excimer formation. Org Lett 2009;11:3378–81.
[22] Xu Z, Yoon J, Spring DR. A selective and ratiometric Cu2+ fluorescent probe based on naphthalimide excimer–monomer switching. Chem Commun 2010; 46:2563–5.
[23] Kim HJ, Park SY, Yoon S, Kim JS. FRET-derived ratiometric fluorescence sensor for Cu^{2+}. Tetrahedron 2008;64:1294–300.
[24] Lee SY, Kim HJ, Wu JS, No K, Kim JS. Metal ion-induced FRET modulation in a bifluorophore system. Tetrahedron Lett 2008;49:6141–4.
[25] Zhou Z, Yu M, Yang H, Huang K, Li F, Yi T, et al. FRET-based sensor for imaging chromium(III) in living cells. Chem Commun; 2008:3387–9.
[26] Long L, Lin W, Chen B, Gao W, Yuan L. Construction of a FRET-based ratiometric fluorescent thiol probe. Chem Commun 2011;47:893–5.
[27] Han ZX, Zhang XB, Li Z, Gong YJ, Wu XY, Jin Z, et al. Efficient fluorescence resonance energy transfer-based ratiometric fluorescent cellular imaging probe for Zn^{2+} using a rhodamine spirolactam as a trigger. Anal Chem 2010; 82:3108–13.
[28] Sun Y, Zhong C, Gong R, Mu H, Fu E. A ratiometric fluorescent chemodosimeter with selective recognition for sulfite in aqueous solution. J Org Chem 2009;74:7943–6.
[29] Lakowicz JR. Principles of fluorescence spectroscopy. 2nd ed. New York: Plenum; 1999.
[30] Tolosa L, Nowaczyk K, Lakowicz J. An introduction to laser spectroscopy. 2nd ed. New York: Kluwer; 2002.
[31] Zhang X, Xiao Y, Qian X. A ratiometric fluorescent probe based on fret for imaging Hg^{2+} ions in living cell. Angew Chem Int Ed 2008;47:8025–9.
[32] Shang GQ, Gao X, Chen MX, Zheng H, Xu JG. A novel Hg^{2+} selective ratiometric fluorescent chemodosimeter based on an intramolecular FRET mechanism. J Fluoresc 2008;18:1187–92.
[33] Atilgan S, Ozdemir T, Akkaya EU. Selective Hg(II) sensing with improved Stokes shift by coupling the internal charge transfer process to excitation energy transfer. Org Lett 2010;12:4792–5.
[34] Suresh M, Mishra S, Mishra SK, Suresh E, Mandal AK, Shrivastav A, et al. Resonance energy transfer approach and a new ratiometric probe for Hg^{2+} in aqueous media and living organism. Org Lett 2009;11:2740–3.
[35] Kim HN, Lee MH, Kim HJ, Kim JS, Yoon J. A new trend in rhodamine-based chemosensors: application of spirolactam ring-opening to sensing ions. Chem Soc Rev 2008;37:1465–72.
[36] Beija M, Afonso CAM, Martinho JMG. Synthesis and applications of rhodamine derivatives as fluorescent probes. Chem Soc Rev 2009;38:2410–33.
[37] Liu B, Tian H. A selective fluorescent ratiometric chemodosimeter for mercury ion. Chem Commun; 2005:3156–8.
[38] Liu B, Tian H. A ratiometric fluorescent chemosensor for fluoride ions based on a proton transfer signaling mechanism. J Mater Chem 2005;15:2681–6.
[39] Lu ZJ, Wang PN, Zhang Y, Chen JY, Zhen S, Leng B, et al. Tracking of mercury ions in living cells with a fluorescent chemodosimeter under single- or two-photon excitation. Anal Chim Acta 2007;597:306–12.
[40] Hanaoka K, Muramatsu Y, Urano Y, Terai T, Nagano T. Design and synthesis of a highly sensitive off-on fluorescent chemosensor for zinc ions utilizing internal charge transfer. Chem Eur J 2010;16:568–72.
[41] Huang J, Xu Y, Qian X. A red-shift colorimetric and fluorescent sensor for Cu^{2+} in aqueous solution: unsymmetrical 4,5-diaminonaphthalimide with N-H deprotonation induced by metal ions. Org Biomol Chem 2009;7: 1299–303.
[42] Xu Z, Xiao Y, Qian X, Cui J, Cui D. Ratiometric and selective fluorescent sensor for Cu^{2+} based on internal charge transfer (ICT). Org Lett 2005;7:889–92.
[43] Xu Z, Pan J, Spring DR, Cui J, Yoon J. Ratiometric fluorescent and colorimetric sensors for Cu^{2+} based on 4,5-disubstituted-1,8-naphthalimide and sensing cyanide via Cu^{2+} displacement approach. Tetrahedron 2010;66:1678–83.
[44] Xu Z, Baek KH, Kim HN, Cui J, Qian X, Spring DR, et al. Zn^{2+}-triggered amide tautomerization produces a highly Zn^{2+}-selective, cell-permeable, and ratiometric fluorescent sensor. J Am Chem Soc 2010;132:601–10.
[45] Kumar M, Kumar N, Bhalla V, Singh H, Sharma PR, Kaur T. Naphthalimide appended rhodamine derivative: through bond energy transfer for sensing of Hg^{2+} ions. Org Lett 2011;13:1422–5.
[46] Yang YK, Yook KJ, Tae J. A rhodamine-based fluorescent and colorimetric chemodosimeter for the rapid detection of Hg^{2+} ions in aqueous media. J Am Chem Soc 2005;127:16760–1.
[47] Zou Q, Tian He. Chemodosimeters for mercury(II) and methylmercury(I) based on 2,1,3-benzothiadiazole. Sensor Actuator B Chem 2010;149:20–7.
[48] Leng B, Jiang J, Tian H. A mesoporous silica supported Hg^{2+} chemodosimeter. AIChE J 2010;56:2957–64.
[49] Guo Z, Zhu W, Zhu M, Wu X, Tian H. Near-infrared cell-permeable Hg^{2+}-selective ratiometric fluorescent chemodosimeters and fast indicator paper for $MeHg^{2+}$ based on tricarbocyanines. Chem Eur J 2010;16:14424–32.
[50] Zhou Y, Xiao Y, Chi S, Qian X. Isomeric boron-fluorine complexes with donor-acceptor architecture: strong solid/liquid fluorescence and large Stokes shift. Org Lett 2008;10:633–6.
[51] Yang XF, Guo XQ, Zhao YB. Development of a novel rhodamine-type fluorescent probe to determine peroxynitrite. Talanta 2002;57:883–90.
[52] Yu H, Xiao Y, Guo H, Qian X. Convenient and efficient FRET platform featuring a rigid biphenyl spacer between rhodamine and BODIPY: transformation of 'turn-on' sensors into ratiometric ones with dual emission. Chem Eur J 2011; 17:3179–91.